J Mater Sci: Mater Electron (2015) 26:4730–4745
DOI 10.1007/s10854-015-3016-1

Recent progresses on hybrid micro–nano filler systems for electrically conductive adhesives (ECAs) applications

Behnam Meschi Amoli[1,3,4] · Anming Hu[5] · Norman Y. Zhou[2,3,4] · Boxin Zhao[1,3,4]

Received: 1 February 2015 / Accepted: 27 March 2015 / Published online: 7 April 2015

Abstract During the last two decades, considerable efforts have been made to explore new generations of interconnecting materials and printed lines to replace the traditionally used toxic lead-based solders in electronic packaging industries. Accordingly, development of electrically conductive adhesives (ECAs) with high electrical conductivity has become an interesting and urgent research venue in this field. Recently, the incorporation of nano-sized conductive fillers inside the conventional formulation of ECAs has drawn considerable attention as an attempt to increase their electrical conductivity. In this article, we review different types of nanofillers that have been utilized inside the conventional ECAs to improve the electrical conductivity of ECAs. We focus on the synergetic effects of silver flakes and the nanofillers on electron transportation through the electrical network; the mechanisms of electrical conductivity enhancement are discussed. Special attention is given to the surface properties of the nanofillers and their corresponding influences on the filler–filler interaction, which has direct effect on the final electrical performance of the hybrid ECAs.

✉ Boxin Zhao
zhaob@uwaterloo.ca

1 Department of Chemical Engineering, University of Waterloo, 200 University Avenue West, Waterloo, ON N2L 3G1, Canada

2 Department of Mechanical and Mechatronics Engineering, University of Waterloo, 200 University Avenue West, Waterloo, ON N2L 3G1, Canada

3 Waterloo Institute for Nanotechnology, University of Waterloo, 200 University Avenue West, Waterloo, ON N2L 3G1, Canada

4 Centre for Advanced Materials Joining, University of Waterloo, 200 University Avenue West, Waterloo, ON N2L 3G1, Canada

5 Department of Mechanical, Aerospace and Biomedical Engineering, University of Tennessee Knoxville, 1512 Middle Drive, Knoxville, TN 37996, USA

1 Introduction

Lead-based solders are the traditional interconnection materials in electronic industries which provide electrical pathways between one circuit element and another upon their attachment to a system level board. However, lead is a health threat for human beings and the environment. The lead-based solders are mainly consumed in the production of electronic devices, which usually possess a life-time of <5 years, which leads to a huge amount of lead accumulation in landfills each year [1]. Many countries have started to establish restricted regulations to abandon the application of lead in their electronic industries [1]. Accordingly, considerable efforts have been conducted to find proper alternatives for these solders.

Today's blooming electronic technologies, e.g., multilayer printed circuits [2], thin-film transistors (TFTs) [3], transparent conductive coating [4], and solar cells [5] require advanced materials that offer high electrical conductivity, good flexibility, proper strechability, and satisfied mechanical strength. In addition, these materials should be cost effective, environmentally benign, and easy processable. In this regard electrical conductive adhesives (ECAs) are considered as one of the most feasible alternative interconnection materials for future applications [6].

ECAs consist of a polymeric matrix, granting the physical and mechanical properties, and conductive fillers, providing electrical pathways throughout the matrix. Depending on the applications and desired properties,

different types of polymers and conductive fillers can be implemented. The conventional ECAs, (which already have found their way into market), are usually based on epoxy as the polymeric matrix and silver flake as the conductive filler. Epoxy provides excellent adhesion, low shrinkage, superior resistance to thermal and mechanical shocks, and have reasonable cost [7]. On the other hand, different types of metallic particle such as copper, nickel, and silver have been used as the conductive filler inside the formulation of ECAs [8–11]. However, silver flake (due to its excellent electrical and thermal conductivities at room temperature, easy processability, and the conductive nature of its oxide) has been the first and foremost utilized conductive filler inside the conventional ECAs [7].

Although conventional ECAs (epoxy + silver flakes) offer several advantages over the traditional lead-based solders, including environmental friendliness, finer pitch printing capability, milder operating condition, fewer processing steps, and more flexibility, [12, 13], the complete replacement of the traditional solders with the conventional ECAs has not yet been achieved because of their poor electrical conductivity. Despite all the progresses, the electrical conductivity of the conventional ECAs (10^{-3}–10^{-4} Ω cm) is still less than that of the eutectic lead-based solders ($\approx 2 \times 10^{-5}$ Ω cm). This situation is elucidated with their different working mechanism. In an ECA, electrons are transferred through the electrical network via the contact points between conductive fillers or by tunneling effect. On the other hand, the eutectic solders work based on solder reflow in which current is passed through the metallic bond [14]. In contrast to soldering, silver flakes inside the epoxy cannot render the metallurgical pathways for electron transportation as metal solders do, but form a small contact point via the formation of a percolated network, which is more difficult for electrons to be transferred through.

It may seem by loading more silver flakes into epoxy the electrical conductivity of the conventional ECAs will increase. However, after the percolation threshold the electrical network becomes stable and adding more silver flakes to epoxy no longer affects the electrical conductivity significantly. Besides, in order to fully replace traditional solders with ECAs, the satisfied electrical conductivity and good adhesive strength should be combined [2, 15, 16]. Adding more filler into epoxy decreases the mechanical strength of the final composite (due to the decreased volume faction of the polymeric matrix) and also negatively influences the processability, and the final cost of the composite [17].

In response to these concerns, the research activities have moved forward towards implementing hybrid filler systems (i.e., the combination of conductive nanofillers and micron-size silver flakes), inside the formulation of ECAs [14, 18–20]. The utilization of nano-sized conductive materials can enhance the electrical conductivities of ECAs at lower filler content without sacrificing the mechanical and adhesive properties. Since the electrons are transferred through the electrical pathways inside epoxy and these pathways are formed via the linkage of conductive filler, the network morphology and quality of contact between neighboring fillers are crucial issues affecting the final electrical performance of the hybrid ECAs [21]. To harness the characteristic properties of the nanosized materials, different parameters such as their size, aspect-ratio, morphology, surface properties, the ratio of silver flakes to nanofillers, and the dispersion techniques should be carefully taken under consideration.

In this article, we review and study the different types of hybrid filler systems that have been utilized inside the formulation of ECAs to improve the electrical conductivity. We shed light on how nanofiller's size, aspect-ratio, morphology, and surface property influence the electrical conductivity of the ECAs. The main focus is on the synergetic effect of the nanofillers and silver flakes as well as the mechanism of electrical conductivity enhancement of the ECAs via the use of the hybrid filler system.

2 Electron transferring mechanism inside ECAs

The mechanism of electron transferring in an ECA is usually explained by the percolation theory [22]. For each ECA, a specific concentration is defined as "percolation threshold". It is the concentration in which a continuous linkage of conductive particles occurs. Following the addition of conductive fillers to a resin, the electrical resistance of ECA slowly decreases until the percolation point. Before percolation, there is no practical connection between fillers. After the percolation threshold, resistance drops abruptly while beyond that, adding more filler does not significantly decrease the resistance [23]. The schematic of relation between the electrical resistivity of an ECA and filler content according to the percolation theory is shown in Fig. 1.

The percolation value depends on different parameters such as size [24], shape [25], nature [26], and the dispersion state of conductive fillers. Each parameter influences the quality of conductive filler linkage in electrical network differently. The size of conductive fillers and their size distribution are important parameters on percolation threshold concentration. Wu et al. [24] filled epoxy with Ag NPs with different sizes (5–1000 nm) and studied the effect of the size of NPs on the percolation value. They observed as the NPs size increased from 5 to 50 nm the percolation concentration decreased to a minimum value of 63 wt%, which was 10 wt% less than that of the

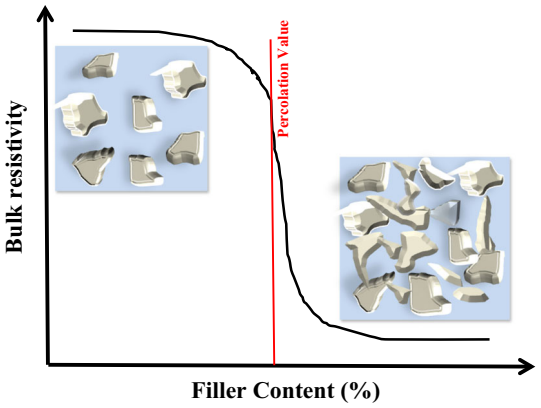

Fig. 1 Typical percolation curve for an ECA based on the percolation theory

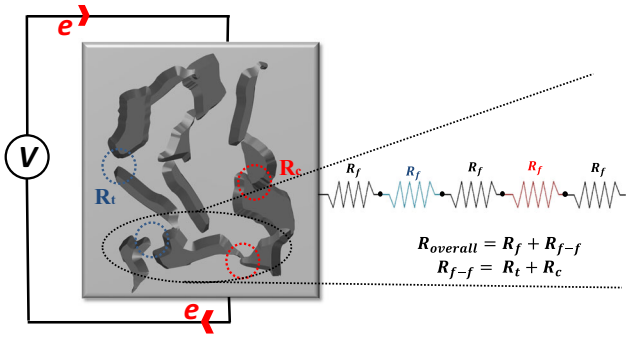

Fig. 2 The mechanism of electrical conduction in an ECA; R_f, R_t, and R_c are the bulk filler, tunnelling and constriction resistances, respectively

conventional ECAs filled with micron-sized Ag particles. However, for the NPs bigger than 50 nm, the percolation concentration increased. Li and Morris [27] performed a two- and three-dimensional computer simulations to predict the effect of particle size distribution on the percolation concentration and reported that the percolation value decreases with broad particle size distribution. The percolation concentration also depends on the morphology of conductive fillers. Lower percolation threshold can be obtained using a high aspect-ratio filler because they can provide more connected pathways at lower filler content [25, 27]. The dispersion state of conductive fillers also has a significant effect on the percolation value. Presence of agglomerations in some level can be useful to form a percolated network at lower filler contents [28]. Li et al. [29] prepared nanocomposites of CNT and epoxy using four different preparation conditions to provide different dispersion states of CNTs inside epoxy. They reported the percolation thresholds ranged between 0.1 and 1 wt% in which the lowest value belonged to the nanocomposite with the second poorest dispersion state. They observed the composite with the best dispersion state did not show any conductivity.

According to percolation theory, electrons are transferred through electrical pathways provided via the filler connections. Figure 2 schematically shows the mechanism of electron conduction throughout the electrical network. The overall resistance of an ECA can be considered as the summation of a series of resistivities, including the bulk resistance of filler (R_f), and filler–filler contact resistance (R_{f-f}) [27, 30].

$$R_{overall} = R_f + R_{f-f} \tag{1}$$

For a specific filler system, the contact resistance (R_{f-f}) is the dominant factor affecting the overall resistance of an ECA. Therefore, to improve the electrical conductivity of ECAs with a specific material as conductive filler, the most effective way is to decrease the contact resistance between neighbouring fillers [1]. The contact resistance itself is the summation of two basic resistances; "constriction resistance", and "tunnelling resistance" [31]. The former, indicated by red circles in Fig. 2, is related to the restriction against free flow of electrons through sharp contact points; the fewer number of contact points in the electrical pathway, the less constriction resistance. Compared to smaller ones, larger particles provide lower number of contact points and larger contact area for electrons transportation inside the network [30]. Hence, micron-sized fillers, e.g., silver flakes, are preferred to be used as the main filler of ECAs. On the other hand, the tunnelling resistance caused by the spots where there are no direct connection between conductive fillers in close proximity (as pointed by blue circles in Fig. 2); and, electrons need to overcome a barrier energy to transfer through the network. This energy causes the tunnelling resistance. For a specific nanofiller, a cutoff distance is defined for the tunnelling effect, in which the resistance between two neighboring fillers is 30 times higher than the bulk resistance of a single nanofiller [32]. The cutoff distance (C) varies for different types of nanofillers. For example, the cutoff distance for Ag NWs is approximately 150 nm, while it is 1 nm for carbon nanotubes (CNTs) [33]. When the center line of two neighboring non-contact nanofillers (d) is larger than their diameter (D) and smaller than or equal to a cutoff distance, $D < d \leq C$, tunnelling of electrons occurs. Simmons [34] derived a generalized formula to quantify the tunnelling effect between similar electrodes, separated by a thin insulating film. Based on his method, the tunnelling resistance for two adjacent non-contact Ag NWs or CNTs can be approximately calculated as [32]:

$$R_{tunnel} = \frac{V}{AJ} = \frac{h^2 d}{Ae^2\sqrt{2m\lambda}} exp\left(\frac{4\pi d}{h}\sqrt{2m\lambda}\right) \tag{2}$$

where V is the potential difference, A is the cross-sectional area, J is the tunnelling current density, h is the Planck's

constant, e is the electron charge, m is the mass of electron, and λ is the height of the barrier energy (for epoxy is 0.5–2.5 eV). The barrier energy depends on the materials that insulate the surface of the Ag NWs (e.g., the polymeric matrix, covering layer, or contamination on the surface of fillers).

3 Electrical conductivity measurement of ECAs

The most important function of an ECA is to form electrical connections with desired conductivity between different electronic parts to form a circuit. Hence, the main focus of the researcher working in this field is to decrease the electrical resistivity of ECAs (close to that of traditional eutectic lead-based solders). Utilization of proper electrical resistivity measurement techniques is of significant importance to examine the efficiency of an ECA. There are two common ways to measure the electrical resistivity of an ECA: two-terminal (2T) sensing and four-terminal (4T) sensing methods. Figure 3 schematically shows the circuit configuration for each method. The 2T sensing method consists of a circuit in which current passes through both the resistor and the voltmeter (Fig. 3a). In this method, the measured voltage is the summation of the voltage drop in the resistor as well as the voltage drop in other parts of the circuit. This method is useful for the applications where high accuracy is not needed.

However, 4T sensing (which is so called Kelvin method) is often employed when high accuracy and optimum performances are required. This method of measurement eliminates inaccuracy attributed to wire resistances, which can be significant in very low resistivities. Figure 3b shows the connections of 4T sensing method, which enables the voltage drop measurements exclusively across the resistor. The voltage circuit has high impedance so that it draws no significant current. Since no current passes through the voltage sensor, one can measure the voltage drop between points a and b (resistor), exclusively (see Fig. 3).

The electrical resistivity measurement of ECAs is usually based on 4T sensing method rather than 2T sensing method. The four-point probe machine is often utilized for this purpose. In this technique, four probes touch the sample surface in which two of the probes are used to apply a specific amount of current through the sample while the others measure the voltage using a high impedance voltmeter (Fig. 4). This method of measurement eliminates different sources of errors such as the probe resistance, the spreading resistance under each probe, and the contact resistance between each probe and samples.

In 1957, Smits developed analytical calculations to evaluate correction factors for the bulk resistivity measurements on infinite and finite sheets using a four-point probe machine. According to his work, in an infinite sheet, a current source is caused a rise to the logarithmic potential,

$$\varphi - \varphi_0 = -\frac{I\rho_s}{2\pi}\ln r \tag{3}$$

where φ is the potential, I the current, ρ_s the sheet resistivity, and r the distance from the current source. In particular, for a dipole (+ source and − source), Eq. 3 can be rewritten as:

$$\varphi - \varphi_0 = \frac{I\rho_s}{2\pi}\ln\frac{r_1}{r_2} \tag{4}$$

For a four-point probe on a sheet, the two outside probes (current) are considered as the dipole. Therefore, the potential difference between the two inner probes (voltage) with equal point spacing for an infinite sheet is:

$$\Delta\varphi = V = \frac{I\rho_s}{\pi}\ln 2 \tag{5}$$

Thus, the sheet resistivity can be calculated as:

$$\rho_s = \frac{V}{I}\frac{\pi}{ln2} = \frac{V}{I}4.53\ldots \tag{6}$$

For a finite sheet with nonconductive boundaries Eq. 6 is rewritten as:

$$\rho_s = \frac{V}{I}C \tag{7}$$

where C is a shape correction factor and depends on (a/d) and (d/s) ratios; where a and d are the length and width of the sheet, respectively, and s is the spacing between the probes (Fig. 4). Table 1 presents the shape correction factor (C) for the sheet resistivity measurements of finite sheets.

For a sample with a finite thickness of w, the voltage gradient, perpendicular to the surface, must be considered while these gradients are negligible for a sheet with $w \to 0$. Smits related the bulk resistivity of an infinite sheet with a finite thickness of w to ρ_s as:

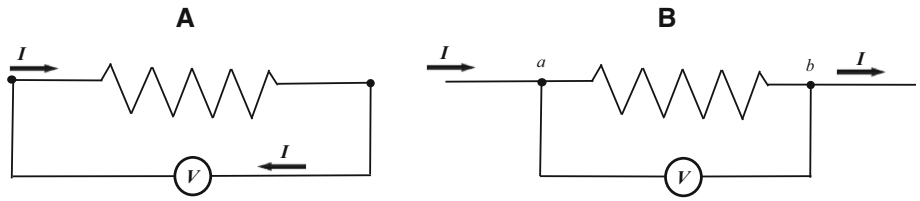

Fig. 3 The circuit configurations of **a** two-terminal and **b** four-terminal sensing method

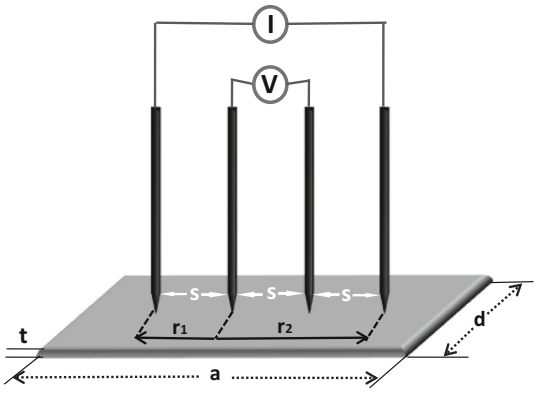

Fig. 4 The configuration of a four-point probe technique for electrical conductivity measurements

Table 1 The shape correction factor (C) for sheet resistivity measurement of finite sheets with four-point probe technique

d/s	$a/d = 1$	$a/d = 2$	$a/d = 3$	$a/d \geq 4$
1.0			0.9988	0.9988
1.25			1.2464	1.2464
1.5		1.4788	1.4893	1.4893
1.75		1.7196	1.7238	1.7238
2.0		1.9454	1.9475	1.9475
2.5		2.3532	2.3541	2.3541
3.0	2.4575	2.7000	2.7005	2.7005
4.0	3.1137	3.2246	3.2248	3.2248
5.0	3.5098	3.5749	3.5750	3.5750
7.5	4.0095	4.0361	4.0362	4.0362
10.0	4.2209	4.2357	4.2357	4.2357
15.0	4.3882	4.3947	4.3947	4.3947
20.0	4.4516	4.4553	4.4553	4.4553
40.0	4.5120	4.5129	4.5129	4.5129
∞	4.5324	4.324	4.5325	4.5324

$$\rho = \rho_s w = \frac{V}{I} w \frac{\pi}{ln\,2} F\left(\frac{w}{s}\right) \tag{8}$$

where F is the correction factor for the bulk resistivity measurement of a finite sheet, and its value depends on the ratio of w/s, as listed in Table 2.

For a finite slice with the thickness of w, the shape correction factor, C, must be added to the Eq. 8

$$\rho = \rho_s \frac{V}{I} wCF\left(\frac{w}{s}\right). \tag{9}$$

For $0.4 \leq w/s \leq 1$, F is close to 1.

4 Electrical conductivity improvement of ECAs

Since the invention of ECAs in 1950 [23], different approaches such as increasing the shrinkage of epoxy [35], surface engineering of silver flakes [36–38], adding low melting component to provide metallurgical connection between silver flakes [39], and addition of nano-size conductive materials to the formulation of conventional ECAs [14, 19, 24, 30, 40–42], have been taken to improve the electrical conductivity of ECAs. Each approach is an attempt to decrease either the constriction or tunnelling resistances.

Table 2 Correction factor (F) for bulk resistivity measurement of finite sheets with the thickness of w using four-point probe

w/s	F (w/s)
0.4	0.9995
0.5	0.9974
0.5555	0.9948
0.6250	0.9898
0.7143	0.9798
0.8333	0.9600
1.0	0.9214
1.1111	0.8907
1.25	0.8490
1.4286	0.7938
1.6666	0.7225
2.0	0.6336

The extensive progresses in nanotechnology have inspired intensive interests to design different types, shapes, and surface chemistries of nano-size materials. Owing to the exceptional and fascinating characteristics of these nanomaterials, the introduction of nano-size conductive fillers inside the conventional ECAs has attracted considerable attentions to improve the electrical conductivity of ECAs. The size [14, 24], morphology [25], surface property [18, 19, 43], and even the type of conductive nanofillers [44] differently impact the final electrical conductivity of ECAs by influencing the contact resistance inside the electrical network. In the following, we review and discuss the recent research activities, which employed nano-size conductive materials (spherical Ag NPs, high aspect-ratio silver nanofillers, and graphitic nanomaterials) as auxiliary filler inside the conventional ECAs to develop new generations of hybrid ECAs.

4.1 Spherical Ag NPs

The incorporation of spherical Ag NPs to the system of epoxy and silver flakes has been practiced by many research groups to develop new hybrid filler systems [19, 24, 41, 45]; however, the role of NPs in modulating the electrical conductivity of ECAs is still controversial. Generally, it has been believed that adding Ag NPs at concentrations less than the percolation value improves the electrical conductivity of ECAs. Lee et al. [46] reported a positive effect of Ag NPs on electrical conductivity when the filler concentration is less than the percolation threshold. Since

at concentrations less than percolation value, silver flakes are not completely connected, the electron tunnelling is the dominated mechanism for electron transferring inside the network. Spherical NPs or their cluster by placing between separated flakes can provide more electrical pathway inside the network, which in turn reduce the tunnelling resistance.

On the other hand, simply adding Ag NPs after the percolation concentration may cause negative effects on the electrical conductivity. In the previously mentioned study, the NPs decreased the electrical conductivity beyond the percolation threshold. Fan et al. [47] and Mach et al. [48] also reported that Ag NPs have negative effects on the electrical conductivity of a system of silver flakes and epoxy at concentrations near or beyond the percolation threshold. This situation can be explained by the concept of the constriction resistance [18]. As mentioned before, constriction resistance is one of the parameters affecting the total resistance of an ECA. This resistance is due to the restrictions against the free flow of electrons through a sharp contact point. The higher number of contact points result in the higher constriction resistance. Addition of NPs increases the number of contact points among fillers in the electrical network, which in turn increases the contact resistance. Furthermore, the large amount of NPs (compared to silver flakes content) may increase the spacing gap between silver flakes and hinder their effective contacts, resulting in lower electrical conductivity values [49].

It should be noted that the most research works, which were carried out to investigate the effect of Ag NPs on the electrical properties of ECAs, used NPs larger than 20 nm (see Table 3). However, it has been reported that very small Ag NPs (i.e., <10 nm), can have positive effects on the electrical conductivity of ECAs, even beyond the percolation content [14, 18]. Very small NPs increase the surface area for electron transportation inside the electrical network by filling the gaps and interstitial spaces between larger silver flakes (see Fig. 5a). In a study by Jeong et al. [14], the positive effect of very small Ag NPs (i.e., 5 nm) on the electrical conductivity of ECAs at concentrations higher than percolation threshold was reported. Using SEM images (Fig. 5b), they stated that small Ag NPs filled the interstices between silver microparticles, which resulted in a low bulk resistivity of 8×10^{-6} Ω cm for the ECAs filled with 92 wt% of silver powder.

4.1.1 *Sintering or metallurgical contact among silver flakes and NPs*

As mentioned before, the increased number of contact points inside the electrical network is a challenge when using Ag NPs inside the ECA formulation. Sintering between Ag NPs is a potential approach to resolve this issue [18, 19, 50–52]. Sintering is a method to form an object from its powder based on diffusion between surface atoms. For metallic particles, the atoms near the surface have fewer bonds with one another, thus less energy is needed for them to leave the surface [53, 54]. For metallic NPs, possessing a large surface area per given volume, the majority of atoms are on the surface; this situation allows them to be sintered at temperatures far lower than their bulk melting temperature. This phenomenon is called the "depressed melting point effect" [55, 56]. Owing to this interesting property, it is possible to form an electrical network with metallurgical connections between fillers by incorporating metallic NPs inside the conventional formulation of ECAs where the formation of metallurgical contact between silver flakes at low temperatures is not possible. As schematically shown in Fig. 6a, sintering not only decreases the number of contact points between fillers, but also increases the contact area of electron transferring. Triggering sintering inside ECAs significantly helps to achieve higher electrical conductivity at low temperatures. Jiang et al. [19] reported an electrical

Table 3 A comparison between different ECAs with hybrid filler systems of micro/nano silver particles

Research groups	r_1 (wt%)[a]	r_2 (wt%)[b]	NP size (nm)	NP surface modification	r_3 (wt%)[c]	Bulk resistivity (Ω cm)
Lee et al. [46]	–	98.2	50	None	98.2	1.93×10^{-4}
Fan et al. [47]	77.5	2.5	55	None	80	10^{-4}
Mach et al. [48]	75	3.5	80–100	None	~79	0.02
Jeong et al. [14]	90	2	5	None	92	8×10^{-6}
Amoli et al. [18]	53	11	<5	Thiocarboxylate group	64	2×10^{-3}
Jiang et al. [19]	48	32	16	Carboxylate group	80	5×10^{-5}
Jiang et al. [30]	–	70	N/A	N/A	70	2.4×10^{-4}
Gao et al. [50]	80	N/A	20–30	None	N/A	7.5×10^{-5}
Zhang et al. [41]	48	32	40–50	Carboxylate group	80	4.8×10^{-5}

[a] r_1: micron-sized silver filler content

[b] r_2: silver NPs content

[c] r_3: total silver content

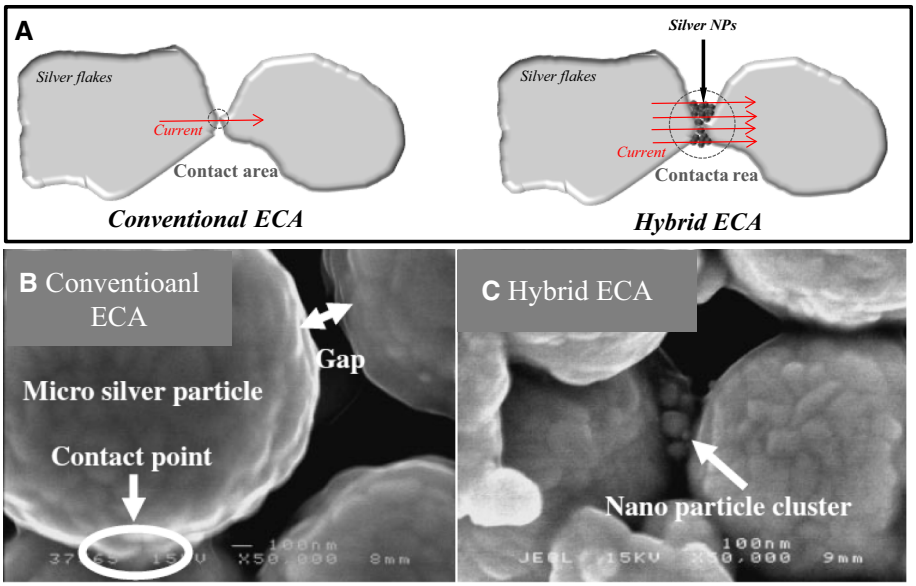

Fig. 5 **a** The mechanism of electron conduction in conventional and hybrid ECAs, **b** an SEM image of a conventional ECA showing a gap between two silver micron-sized particles, **c** an SEM image of a hybrid filler system showing Ag NPs filling the gap between two silver particles (**b**, **c** reproduced by permission from Materials Transactions copyright) [14]

resistivity of 5×10^{-5} Ω cm upon the incorporation of carboxylate functionalized Ag NPs to the system of silver flakes and epoxy (with total filler content of 80 wt%). They related the low electrical resistivity to the sintering of NPs at low curing temperature of 150 °C. Figure 6b, c shows NPs morphological change after sintering.

The thermodynamic driving force for particle sintering of any size is based on the reducing their surface energy, which can be expressed by Fang and Wang [57]:

$$\sigma = \gamma K = \gamma\left(\frac{1}{R_1} + \frac{1}{R_2}\right) \tag{10}$$

where γ is the surface energy, K is the curvature of a surface, and R_1 and R_2 are the principle radii of the curvature. For a convex surface, the curvature is taken to be positive whereas for a concave surface is negative. According to Eq. 10, the driving force of particles sintering is inversely proportional to their size. Therefore, the driving force for the sintering of nano-sized particles is significantly larger than micro-sized particles. Apart from the surface energy driving force, there is another driving force for particle sintering, which is related to mass transport phenomenon. The mass transport, occurring during sintering, is driven by the difference in vacancy concentration

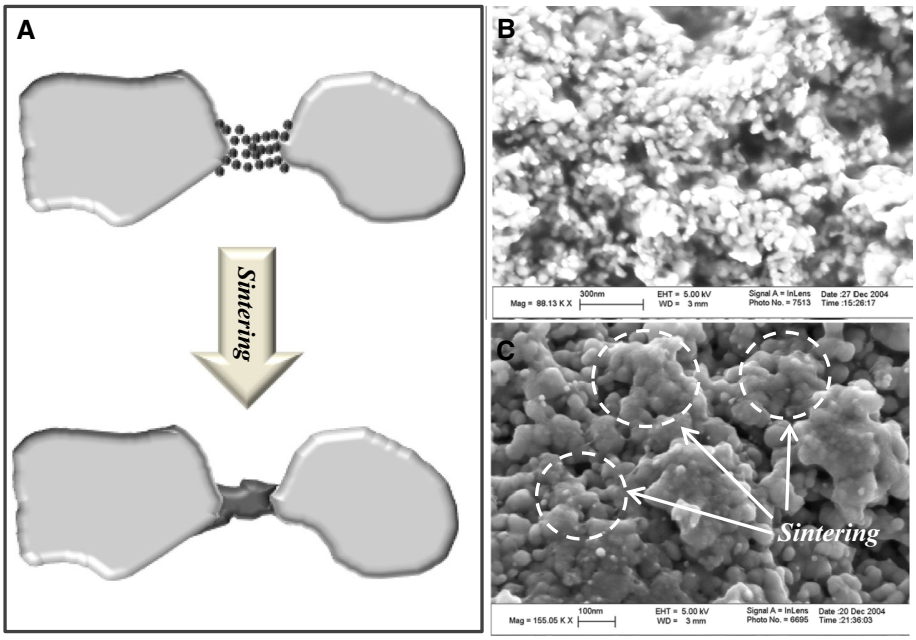

Fig. 6 **a** The schematic of sintering between Ag NPs, **b** Ag NPs before sintering, and **c** after sintering (**b**, **c** have been reproduced from copyright Springer) [30]

$(\Delta C_v = C_v - C_{v0})$, where C_v is the vacancy concentration of a surface with the curvature of K, and C_{v0} is the vacancy concentration of a flat surface. The relation between C_v and C_{v0} is defined by Gibbs–Thomson equation:

$$C_v = C_{v0} \exp\left(-\frac{\gamma K \Omega}{kT}\right) \tag{11}$$

where Ω is the atomic volume, k is Boltzmann's constant, and T is the absolute temperature. For micron-size particles, the term $\left(\frac{\gamma K \Omega}{kT}\right)$ is very smaller than 1, and $C_v \approx C_{v0}\left(1 - \frac{\gamma K \Omega}{kT}\right)$, accordingly ΔC_v is equal to:

$$\Delta C_v \approx -C_{v0} \frac{\gamma K \Omega}{kT} \tag{12}$$

However, for nano-size particle, the mass transport driving force is expressed by:

$$\Delta C_v = C_{v0}\left[\exp\left(-\frac{\gamma K \Omega}{kT}\right) - 1\right] \tag{13}$$

Equation 13 shows when the particles size decreases to nanoscale, the mass transport driving force increases exponentially. All in all, the sintering driving force of any particle consists of two distinct parameters: surface energy driving force and mass transport driving force. For nano-size particles, both of these parameters are significantly larger than its micron-size counterpart. This explains why the presence of nano-sized particles is necessary in the system of conventional ECAs to provide metallurgical connections among micron-size silver flakes.

Rather than their size, the sintering of NPs is affected by the covering layer on their surface [30, 58, 59]. NPs without any surface coverage can be sintered to each other even at room temperature [50, 59]. Metallic NPs thermodynamically tend to form aggregates to reduce their surface energy. An organic layer over their surface is required to prevent the aggregation by providing large steric repulsion and also by reducing their surface energy [56]. However, the presence of this organic layer is detrimental to the sintering at low temperatures, which sometimes is a vital requirement for temperature sensitive devises. Hence, to make sintering happen at low temperature, the organic layer should be easily removed from the surface of NPs. The common stabilizing agents, such as polyvinylpyrrolidone (PVP), polyethylene glycol (PEG), long-chain alkanethiol, and amines usually form chemical bonds with NPs surface, which are hard to remove. Besides, in the most cases, a large amount of these stabilizing agents cover the surface of NPs. To detach these organic residues elevated temperatures (i.e., 200 °C or higher) are often needed, which is usually higher than the bearing temperature of the polymeric matrix or the substrate.

Proper surface functionalization techniques can provide a controlled amount of organic material over the NPs surfaces with controlled de-bonding temperature. Many research groups tried to reduce the sintering temperature due to the thermal sensitivity of components in organic electronic devices [41, 45, 50, 51, 60]. For instance, in a study by Zhang et al. [41], they investigated the effect of two different surface covering layers on the sintering temperature of Ag NPs as well as the final electrical resistivity of the nanocomposites. They synthesized Ag NPs using combustion chemical vapour condensation (CCVC) method, which results in lower amount of surface residue on NPs surface compared to the common wet chemistry approaches. They used the same precursor but different reducing atmosphere, which led to the formation of NPs with carboxylate and oxidized surface. They reported that the complete removal of surface residue has a significant influence on the final electrical conductivity of the composite filled with Ag NPs and silver flakes. To study the effect of surface residue on the electrical conductivity, they cured the composites at 180 °C and achieved a bulk resistivity of 4.8×10^{-5} Ω cm for the ECAs filled with 80 wt% of silver (flakes and NPs); this resistivity was three orders of magnitude less than that of the ECAs cured at 150 °C. This electrical resistivity difference is because at 150 °C, some organic residues still remain on the NPs surface, inhibiting their complete sintering. Since carbonaceous residue is partially decomposed from the surface at 180 °C, the ECAs filled with Ag NPs with carboxylate surface showed higher electrical resistivity compared to that filled with the NPs with oxideized surface.

Some research groups tried in situ approaches to synthesize Ag NPs inside epoxy during the curing process to generate Ag NPs without any surface residue enabling sintering at very low temperature. For instance, Gao et al. [50] reported in situ synthesis of Ag NPs inside epoxy (filled with 80 wt% of silver flakes) during the curing process without the use of any stabilizer; they reached to a bulk resistivity of 7.5×10^{-5} Ω cm.

4.1.2 The effect of chain length of covering layer

NPs are usually covered by an organic material to control their shape, property, and also prevent their aggregation in different media. As reinforcing agent in nanocomposite fabrication, NPs are also required to be covered by organic materials to make them compatible with their polymeric host [19]. These layers inhibit the electrical performance of the final composite because of their insulating nature. The chain length of the organic layer over the surface of fillers is a critical parameter influencing the final electrical properties of ECAs; the shorter chain lengths result in more convenient electron transportation than the longer ones. In a study by Li et al. [61], they replaced the commonly used

stearic acid (the covering layer of silver flakes with 18 carbons) by short chain dicarboxylic acids (malonic and adipic acid with 3 and 6 carbons in their backbone, respectively), and reported a significant electrical conductivity improvement. Jiang el al. [30] also studied the effect of the introduction of Ag NPs treated by 5 different surfactants inside epoxy. Their results showed that the surfactant chain length has an important impact on the sintering initiation and consequently the electrical resistivity of ECAs (see Table 3), although it has not been mentioned what kind of surfactants were used.

In our previous work, we synthesized very small Ag NPs (<5 nm) functionalized by two different thiocarboxylic acids with different chain lengths (3 and 11 carbons). We observed that the chain length of acids largely affects the electrical behaviour of the synthesized Ag NPs in which the NPs covered by long-chain acid were electrically insulated, while those covered by short-chain acid were conductive [18]. Subsequently, the conductive NPs were added inside the conventional ECAs, consisted of epoxy and silver flakes. As stated earlier, the size of NPs is one of the important parameters affecting the sintering temperature. Hence, by introducing very small Ag NPs to the formulation of conventional ECAs, one can take advantage of NPs sintering at low temperature (150 °C) while also filling the interstices between silver flakes at the same time. Addition of a small amount of the Ag NPs (weight ratio of Ag NPs–Ag flakes 1:5) to the system reduced the electrical resistivity three orders of magnitude compared to a conventional ECA filled with the same amount of conductive filler.

4.2 High aspect-ratio silver nanofillers

The main drawback of the conventional ECAs is its inability to reach a resistivity below 10^{-4} Ω cm even after using large amounts of silver flakes [6]. On the other hand, by increasing the amount of filler the volume fraction of epoxy decreases; consequently, the adhesive strength of the composite decreases. Recently, high aspect-ratio silver nanofillers are proposed as a promising option to overcome this issue. High aspect-ratio silver nanofillers can establish a percolated network at very low filler content [62, 63]. Compared to spherical Ag NPs, these nanofillers provide lower number of contact points and larger surface area for electron transportation, which in turn decreases the constriction resistance. Besides, the large aspect-ratio of these nanomaterials can provide more electrical paths inside the composite which significantly decreases the electrical resistance (see Fig. 7).

These interesting features of the high aspect-ratio silver nanomaterials have drawn a considerable attention among the active research groups working in this field to exploit them as either the main or auxiliary filler inside the formulation of ECAs. Wu et al. [64] filled epoxy with 56 wt% of Ag NWs and reported four orders of magnitude electrical conductivity improvement compared to that of the ECAs filled with the same amount of macro- and nano-size Ag particles (see Table 4). It should be noted that the shear strength of the ECA filled with NWs was ~17.6 MPa, showing a 0.3 MPa improvement compared to that filled with macro- and nano-size Ag particles. Tao et al. [16] also reported the same results. Yu et al. [65] reported 13 orders of magnitude electrical conductivity improvement via the incorporation of 50 wt% of Ag NWs modified by (3-aminopropyl)triethoxysilane (APTES). They related the electrical conductivity improvement to the homogenous dispersion of NWs inside epoxy, establishing a percolated network at low filler content.

However, the direct addition of high aspect-ratio nanofillers into epoxy requires a large amount of materials to achieve the desired conductivities. Utilization of these nanomaterials as an auxiliary filler in conventional ECA can render a synergetic effect between high aspect-ratio silver nanomaterials and silver flakes to improve the electrical conductivity of the resulting hybrid ECAs. Chen et al. [2] studied the electrical conductivity of a system consisted of silver micron-sized particles, doped with Ag NWs and compared the results with an un-doped system. They reported the doped system showed better electrical conductance compared to un-doped one with the same amount of silver fillers. Using TEM and SEM images, they related the improved electrical conductivity to the bridging of NWs between separated micron-size silver particles. In another work in 2010, they incorporated Ag NWs inside the conventional formulation of ECAs and reported an improved electrical conductivity for the hybrid ECAs compared to the one with Ag NPs as co-filler [66].

4.2.1 Sintering of the high aspect-ratio silver nanofillers

Owing to their nano size scale, high aspect-ratio Ag nanofillers can also provide the advantage of sintering and metallurgical connections between fillers at low temperature because of the "melting point depression effect" [55]. Same as spherical Ag NPs, the surface coverage has an important impact on the sintering temperature. Xiao's research group studied the effect of covering layer on the sintering behaviour of Ag NWs synthesized by a polyol process [67]. They functionalized NWs by a fatty acid (aliphatic acids) and polyvinyl pyrrolidone (PVP). They observed that the NWs functionalized by the fatty acid began to sinter to one another at 200 °C, while sintering did not happen for those covered by PVP. Peng et al. [59] showed that PVP can be washed out from the NWs surface, resulting in a room-temperature sintering of the NWs. In

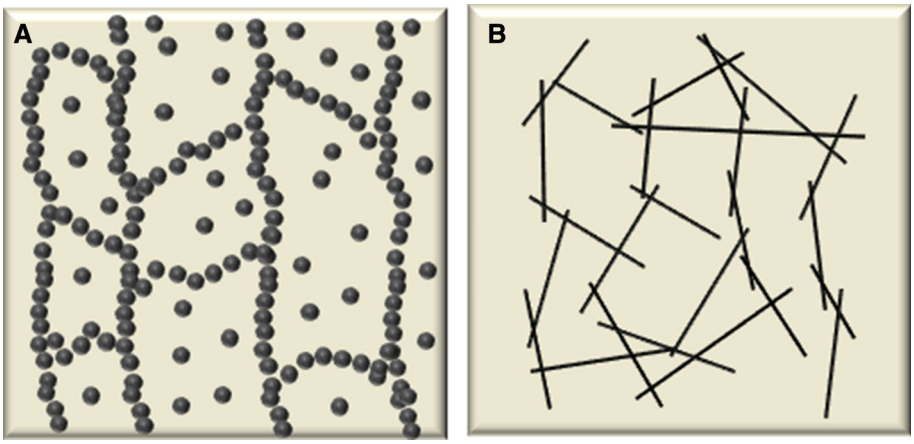

Fig. 7 The establishment of electrical network using **a** silver NPs, and **b** high aspect-ratio silver nanofillers

Table 4 A comparison between ECAs with high aspect-ratio nanofillers

Research groups	Silver flakes (wt%)[a]	Silver NW (wt%)	CNT (wt%)	Graphene (wt%)	Total silver content (wt%)	Bulk resistivity (Ω cm)
Wu et al. [64]	–	56	–	–	56	1.2×10^{-4}
Zhang et al. [67][a]	–	76	–	–	76	7.1×10^{-4}
Zhang et al. [69][b]	45	30	–	–	75	5.8×10^{-6}
Xuechun and Feng [83]	72	–	0.24	–	72	1.43×10^{-3}
Marcq et al. [42]	70	–	0.4	–	70	2×10^{-4}
Wu et al. [84][c]	–	–	41	–	–	2.21×10^{-4}
Oh et al. [85][d]	80	–	2	–	80	1.84×10^{-5}
Oh et al. [21][e]	79.5	–	1.5	–	81	4×10^{-6}
Luan et al. [80]	–	50	–	N/A	50	$\sim 10^{-3}$
Peng et al. [87][f]	65	–	–	15	65	2.37×10^{-4}
Liu et al. [89][g]	80	–	–	0.05	80	4.3×10^{-5}
Liu et al. [88][g]	80	–	–	N/A	80	3×10^{-5}
Amoli et al. [91][h]	80	–	–	1	80	4.5×10^{-5}

[a] The silver NWs were functionalized by an aliphatic acid

[b] The silver NWs were functionalized by dicarboxylic acids (e.g., pentanedioic acid)

[c] The CNTs were coated with silver NPs of 5 nm

[d] The CNTs were covered by silver NPs of 100–200 nm

[e] The CNTs were covered by silver NPs of 20 nm which were functionalized by glutaric acid

[f] The graphene was decorated by silver NPs of ~30 nm

[g] The graphene was decorated by silver NPs of ~10 nm

[h] The graphene was decorated by Ag NPs of small than 5 nm and functionalized with MPA

another work by Xiao's group, they used di-carboxylic acids to functionalize Ag NWs. Di-carboxylic acids (due to their good affinity with metallic surfaces) are commonly used as shielding layer over the surface of Ag NPs to prevent their oxidation [68]. Since they chelate to the NPs surface, they can be easily detached from the surface, enabling the NPs to be sintered at low temperature [19]. They observed that the functionalized NWs started to sinter to each other at 200 °C and gradually became shorter and thicker as temperature increased [69]. To trigger sintering inside ECAs, they incorporated the functionalized NWs into the conventional ECAs and reported an electrical resistivity of 5.8×10^{-6} Ω cm for the epoxy filled with 75 wt% of the modified NWs and silver flakes (with the weight ratio of 2:3) [69].

Although the electrical conductivity improvement of ECAs via introduction of high aspect-ratio silver nanomaterials has been reported, those efforts are mainly limited to the use of Ag NWs. We recently developed a new method to produce a novel type of high aspect-ratio Ag

nanomaterial, i.e., Ag nanobetls (NBs), covered by polymethacrylic acid (PMAA). We indicated that NBs formed based on "self-assembly and room-temperature joining of hexagonal and triangular Ag NPs" (see Fig. 8a). Compared to the commonly used Ag NWs, which are synthesized at high temperature (>60 °C) and requires long reaction time (>1 h) [70], the preparation of the NBs is fast (<10 min) and occurs at room temperature [71]. Because of a low "weight to length" ratio of the NBs, they can form a percolated network at very low filler concentrations. In order to study the effect of the synthesized NBs on the electrical conductivity of ECAs, they were incorporated to the system of silver flakes and epoxy at different silver content ranges (near and beyond the percolation value) [72]. We observed that to improve the electrical conductivity of ECAs, the use of small amount of NBs is more effective than adding more silver flakes to the system; the incorporation of 2 wt% of NBs to the system of silver flakes and epoxy (total silver content of 61 wt%) increased the electrical conductivity 1660 % compared to that of the conventional ECA with the same silver content. As can be observed in Fig. 8b, c, the NBs by bridging between the separated silver flakes made them connected and established more completed network with more electrical pathways inside epoxy. It should be noted that filling the epoxy with 80 wt% of silver flakes and the NBs reduced the bulk resistivity up to 3×10^{-5} Ω cm which is close to that of eutectic solders (2×10^{-5} Ω cm) [6]. We observed that the effect of NBs on the electrical conductivity improvement of ECAs is more pronounced at concentrations close to percolation regions than beyond that. The application of high aspect-ratio silver nanomaterials in the formulation of the ECAs is still in earlier stages and needs to be explored further in either the type of nanofillers or their surface engineering techniques.

4.3 Graphitic nanofillers

Due to the exceptional mechanical and electrical properties of graphitic fillers (i.e., CNTs and graphene), recently a considerable attention has been drawn to utilize these nonomaterials in the field of electrical conductive nanocomposites. CNTs, first identified by Iijima [73], are sheets of graphite, rolled into seamless tube. They are categorized into single wall (SWCNT), double wall (DWCNT), and multi wall (MWCNT) CNTs. On the other hand, graphene nanosheet is a flat monolayer of carbon atoms, 0.335 nm thick, densely packed into a honeycomb two-dimensional (2-D) lattice structure [74]. SWCNTs can be considered as rolls of graphene nanosheets; depending on at which direction they being rolled up, their electrical properties would be different [75]. CNTs and graphene, possessing very large surface area per given volume and very high aspect-ratio can create a percolated electrical network at very low filler content. By introducing these nanomaterials inside conventional ECAs, the density of the final ECAs is decreased significantly [76]. In addition, compared to traditionally use metallic fillers, the

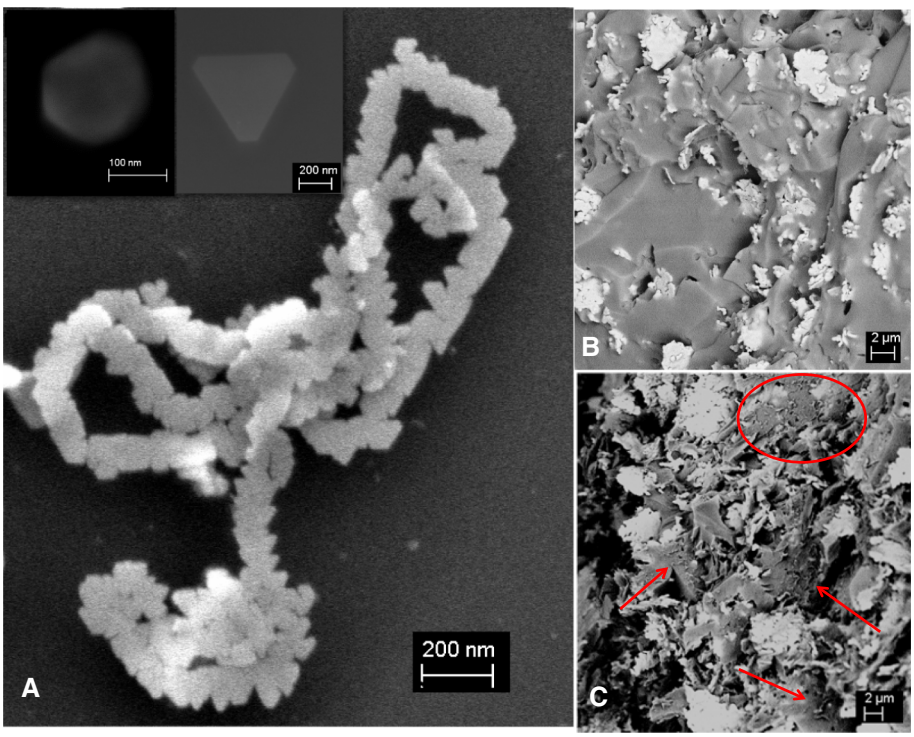

Fig. 8 **a** A SEM images of synthesized silver NBs (the *insets* are the *hexagonal* and *triangular* silver structural blocks of the NBs), **b** a SEM image of the cross-section of the conventional ECA, **c** a SEM image of the cross-section of the hybrid ECA (reproduced by permission from Wiley copyright) [72]

exceptional mechanical properties of these nanomaterials can enhance the mechanical strength of the final ECAs drastically.

To harness the characteristic properties of these nanomaterials they must be efficiently dispersed inside their polymeric host. The bottleneck is that feeding polymers with as-prepared graphitic fillers usually leads to form aggregates as they tend to be held together (by van der Waals forces and/or entanglements) [77]. Stabilization of CNT/graphene by assistance of surfactant in liquid media [78], or surface functionalization via covalent bonding or π stacking [79] are the main possible approaches to disperse and exfoliate these nanomaterials inside a polymeric matrix. Both approaches have some drawbacks. Although the surface modification of graphitic fillers via covalent bonding may lead to better dispersion and interfacial interaction between nanofillers and polymeric chains [80], this method may hinder the electrical performance of nanofillers due to disturbance of π-electron delocalization [77]. On the other hand, dispersion of these nanomaterials by assistance of surfactant in organic solvents preserves their chemical structure. However, some issues challenge this approach for nanocomposite fabrication. First, the best solvents to disperse these nanomaterials have high boiling points and so are difficult to be removed during composite formation. Second, a limited amount of CNT/graphene can be stabilized inside organic solvents by assistance of surfactants [81]. Third, residual surfactant removal is difficult in the most cases [78].

Although some research works have been conducted to fabricate epoxy filled with graphitic fillers [82], the nanocomposites with graphitic nanofillers as the main conductive filler cannot meet the minimum requirements of advanced ECAs. However, their high aspect-ratio along with their conductive nature makes them a perfect option as auxiliary filler in the system of epoxy and silver. In this case, the main part of electrical network is constructed by silver materials and the graphitic fillers help to establish the percolated network while reducing the filler content. In a study by Xuechun and Feng [83], they investigated the effect of MWCNTs on the electrical conductivity of ECAs filled with silver flakes. They used surfactants to dispersed MWCNTs in acetone. The results indicated that adding MWCNTs, especially before percolation threshold, remarkably increased the electrical conductivity while beyond the percolation threshold the influence of MWCNTs on electrical conductivity was not pronounced. Marcq et al. [42] also reported the synergetic effect of CNTs and silver flakes on electrical conductivity improvement of ECAs. Luan et al. [80] filled epoxy with a novel hybrid filler system, consisting of Ag NWs and 2-D chemically reduced graphene sheets (with hydroxyl groups over the surface). They observed that the percolation threshold decreased to a surprising value of 20 wt% and the electrical conductivity remarkably improved (see Table 4). They attributed the electrical conductivity enhancement to the reduction of tunnelling resistance between NWs due to the presence of graphene nano-sheets.

The efficiency of electrical pathways largely depends on the bulk resistivity of conductive fillers as well as the quality of contact between neighbouring fillers. Hence, the surface decoration of graphitic fillers using metallic NPs has been performed by some research groups as an attempt to increase their average electrical conductivity and also to decrease the contact resistance between fillers [21]. Wu et al. [84] decorated MWCNTs by Ag NPs and incorporated them as conductive filler inside epoxy. They also filled epoxy with non-modified MWCNTs. For the ECA filled with decorated MWCNTs they reported a bulk resistivity of 2.21×10^{-4} Ω cm at the percolation content, which showed one order of magnitude electrical conductivity improvement compared to that of the ECAs filled with non-modified MWCNTs at the same concentration (see Table 4). Baik and his co-workers modified the surface of CNTs with carboxylate groups as well as nickel and Ag NPs and incorporated them into commercial silver pastes, consisting of silver flakes and epoxy. No matter which type of surface-modified CNT was added to the paste, the electrical conductivity improved drastically, while addition of the Ag-coated CNTs led to the most improved electrical conductivity (i.e., 83 %) [85] (see Table 4).

It was mentioned that if sintering take place between neighbouring fillers, the contact resistance decreases dramatically. To take advantage of the sintering between fillers, Biak and his co-worker decorated CNTs by Ag NPs functionalized with a di-carboxylic acid [21]. The presence of the di-carboxylic acid on the surface of small NPs prevents their oxidation and also allows the coalescence of NPs at a relatively low temperature of 180 °C. Incorporation of the decorated MWCNTs into the commercial silver paste (81 wt% of conductive filler) decreased the electrical resistivity of the hybrid ECA up to 4×10^{-6} Ω cm, which showed a significant improvement compared to that of the ECAs with non-modified CNTs. They indicated that the self-assembly and coalescence of Ag NPs on the surface of MWCNTs made them more compatible with micron-sized silver flakes. The authors speculated that silver-decorated MWCNTs construct electrical bridges between separated silver flakes during the curing step, and the NPs presented at the end of each tube sintered the MWCNTs to the neighbouring silver flake (see Fig. 9). The metallurgical connections between silver flakes and Ag NP-decorated MWCNTs significantly decrease the electrical resistance and provide more electrical pathways for electrons transportation inside the network.

Graphene nano-sheets also due to their 2-D structure, and higher aspect-ratio compared to CNTs can provide more effective electrical network inside ECAs at very lower filler content. Pu et al. [86] used nitrogen-doped graphene inside the system of epoxy and silver powder and reported that the percolation of silver powder reduced to 30 wt%. Their results confirmed that 2-D graphene is much more effective than other types of high aspect-ratio carbon-based fillers such as CNTs and carbon black. However, the challenge of attaining a homogeneous dispersion, as well as preserving its single-layer structure inside the composite acts as a bottleneck in ECA fabrication. Inspired by the research activities on the metallization of CNTs, some research groups decorated the graphene surface with Ag NPs and used that inside the ECAs formulation. Peng et al. [87], recently reported the electrical conductivity improvement of ECAs via addition of Ag NP-decorated graphene to the conventional ECAs.

If sintering of Ag NPs on the graphene surface occurs, it can significantly decrease the contact resistance between neighboring fillers via the formation of metallurgical contacts between silver flakes and graphene nanosheets. It should be noted that the organic layer over the surface of the Ag NPs has an important impact on their sintering behavior. The smaller amount of organic material and the shorter organic chain length help the sintering at low temperature, as well as electron transferring inside the network. Recently, Liu's research group developed new in situ approaches to decorate the graphene surface with Ag NPs for ECAs application [88–90]. In their method, the formation of Ag NPs on graphene surface occurs during the curing process of epoxy, making the NPs size very sensitive to curing temperature. Although in situ approaches eliminate the use of organic layer over NPs surface, it makes it difficult to keep the NPs size constant as the curing temperature changes. Furthermore, at temperatures less than NPs formation temperature, there would be no Ag NPs inside the nanocomposites, thereby limiting the applications of the ECAs to those operating at temperatures higher than NPs formation temperature.

In our previous work, we employed a simple wet chemistry approach to decorate the graphene surface with Ag NPs for ECA applications and carried out a systematic investigation on the effect of NPs sintering on the electrical conductivity improvement of hybrid ECAs [91]. The NPs were functionalized with MPA to control their size and to prevent their oxidation. By decorating the graphene surface with small size MPA-functionalized Ag NPs and introducing them into epoxy/silver composite, we could provide metallurgical connection between neighboring fillers and also increase the surface area for electron transportation inside the electrical network. The electrical conductivity of the hybrid ECAs were measured at two different curing temperatures (150 and 220 °C) and compared to those of conventional ECAs and hybrid ECAs with non-modified graphene. Our results indicated that the for the ECAs cured at 150 °C, electrical conductivity significantly improved via addition of the decorated graphene at concentration near percolation value, while that improvement was not noticeable at higher filler contents. However, as the curing temperature increased to 220 °C, the electrical conductivity enhancement became more pronounced at higher concentrations. We prepared a highly conductive hybrid ECA by introducing 1 wt% Ag NP-decorated graphene nanosheets into the conventional ECAs. The resultant hybrid ECAs was found to have a bulk resistivity of

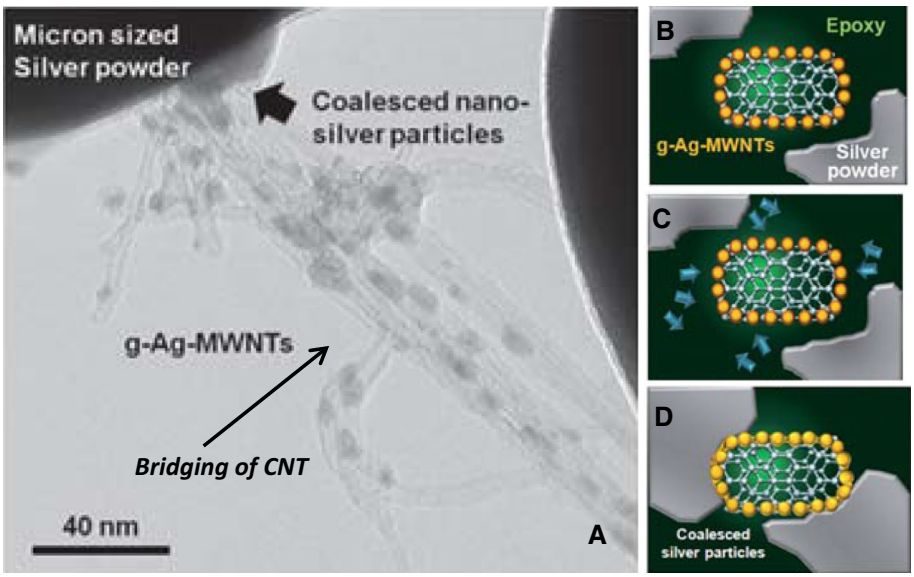

Fig. 9 **a** The bridging of CNT between separated silver flakes without epoxy, **b–d** schematics of electrical network formation via the bridging and coalescence of Ag decorated CNTs between silver flakes (reproduced by permission from RSC copyright) [21]

4.6×10^{-5} Ω cm which is close to that of lead-based solders. We believe that the improved electrical conductivity of ECAs via addition of Ag NP-decorated graphene is mainly because of the reduction of the tunnelling resistance; however, the increased number of contact points (due to the presence of Ag NPs on the graphene surface) may cancel out this positive effect. To decrease the number of contact points sintering of NPs must occur, which requires elevated curing temperatures (higher than 150 °C). We hypothesize that the single layer graphene without metallic decoration should be a better option as auxiliary filler for ECA application if a proper exfoliation technique is applied to preserve its single layer structure within the epoxy matrix.

5 Conclusions and remarks

Versatile and valuable efforts have been made to overcome one of the most challenging issues of ECAs, which is their low electrical conductivity compared to traditional lead-based solders. This review covers one of the main strategies for improving the electrical conductivity of ECAs, which is the incorporation of nano-size conductive material (spherical Ag NPs, high aspect-ratio silver nanofillers, graphitic nanofillers) inside the conventional formulation of ECAs. Followings are the main concluding remarks:

1. One of the most common conductive nanomaterials that have been utilized to improve the electrical conductivity of ECAs is spherical Ag NP. Spherical Ag NPs at concentrations less than percolation threshold have positive effect on the electrical conductivity of the conventional ECAs because of bridging between separated silver flakes and providing more electrical pathways in the system, while beyond that concentration the conductivity decreases because of the increased number of contact points between neighbouring fillers. However, very small NPs (<10 nm) can always improve the electrical conductivity even beyond percolation threshold. This situation occurs because small NPs can fill the gap between silver flakes which increases the contact area of electron transportation.
2. High aspect-ratio Ag nanofillers, e.g., Ag NWs, and Ag NBs, can establish a percolated network at low filler content and provide less number of contact points between fillers along the electrical pathways. The low filler content increases the mechanical strength of ECAs and also decreases its final cost.
3. CNT/graphene, possessing high surface area per given volume, low density and excellent electrical properties, are new classes of auxiliary fillers that can create more electrical pathways inside the network and increase the area of electron transportation. Recently, different approaches have been employed to decorate the surface of these nanofillers with Ag NPs which significantly reduces the contact resistance between fillers. The combination of these nanofillers with silver flakes can decrease the electrical resistivity of the ECAs up to 4×10^{-6} Ω cm.

Although extensive progresses have been made during the last decades to increase the electrical conductivity of ECAs by incorporating nanoscale conductive particles inside the conventional formulation of ECAs, there are some important questions which are still unsolved. In most studies, researchers reported very high electrical conductivity, but the optimum amount of nanofillers is not reported. A systematic study for each type of nanofillers (especially for high aspect-ratio nanofillers) is needed to shed more light on the optimum ratio of micron-size silver flakes to nanofillers which is a critical parameter affecting the quality of filler network as well as the final electrical performance of ECAs. Some research groups studied the effect of NPs surface modifications on the final electrical conductivity of ECAs. However, those studies are discreet and explained specific systems. Further researches must be performed to comprehensively study the effect of surface functionalization on the quality of NPs dispersion inside epoxy, the mechanism of filler interaction with polymeric chains, and their effect on the percolation threshold of ECAs.

Acknowledgments This work was supported by a Strategic Project Grant from the Natural Sciences and Engineering Research Council of Canada (NSERC).

References

1. Y. Li, C.P. Wong, Mater. Sci. Eng. R Rep. **51**, 35 (2006)
2. C. Chen, L. Wang, R. Li, G. Jiang, H. Yu, T. Chen, J. Mater. Sci. **42**, 3172 (2007)
3. H.J. Yun, K.H. Baek, L.M. Do, K.S. Jeong, Y.M. Kim, S.D. Yand, S.Y. Lee, H.Y. Lee, G.W. Lee, J. Nanosci. Nanotechnol. **13**, 3313 (2013)
4. M. Layani, S. Magdassi, J. Mater. Chem. **21**, 15378 (2011)
5. Y. Zemen, S.C. Schulz, H. Trommler, S.T. Buschhorn, W. Bauhofer, K. Schulte, Sol. Energy Mater. Sol. Cells **109**, 155 (2013)
6. C. Yang, C.P. Wong, M.M.F. Yuen, J. Mater. Chem. C **1**, 4052 (2013)
7. Y. Li, D. Lu, C.P. Wong, *Electrical Conductive Adhesives with Nanotechnologies*, 1st edn. (Springer, New York, 2010), pp. 1–19
8. S. Qi, R. Litchfield, D.A. Hutt, B. Vaidhyanathan, C. Liu, P. Webb, S. Ebbens, IEEE 62nd Electron. Compon. Technol. Conf. 1651–1655 (2012)
9. I.N. Kholmanov, S.H. Domingues, H. Chou, X. Wang, C. Tan, J.Y. Kim, H. Li, R. Piner, A.J.G. Zarbin, R.S. Ruoff, ACS Nano **7**, 1811 (2013)
10. I. Halaciuga, J.I. Njagi, K. Redford, D.V. Goia, J. Colloid Interface Sci. **383**, 215 (2012)

11. N. Hansen, D.O. Adams, K.L. DeVries, A. Goff, G. Hansen, J. Adhes. Sci. Technol. **25**, 2659 (2011)
12. S. Bohm, E. Stammen, *Microjoining and Nanojoining* (Cambridge, England, 2008), p. 500
13. S. Nam, H.W. Cho, T. Kim, D. Kim, B.J. Sung, Appl. Phys. Lett. **99**, 043104 (2011)
14. W. Jeong, H. Nishikawa, D. Itou, T. Takemoto, Mater. Trans. **46**, 2276 (2005)
15. K.Y. Chun, Y. Oh, J. Rho, J.H. Ahn, Y.J. Kim, H.R. Choi, S. Baik, Nat. Nanotechnol. **5**, 853 (2010)
16. Y. Tao, Y. Xia, H. Wang, F. Gong, H. Wu, G. Tao, IEEE Trans. Adv. Packag. **3**, 2589 (2009)
17. R. Zhang, J.C. Agar, C.P. Wong, Proc. 12th Electron. Packag. Technol. 696–704 (2010)
18. B.M. Amoli, S. Gumfekar, A. Hu, N.Y. Zhou, B. Zhao, J. Mater. Chem. **22**, 20048 (2012)
19. H. Jiang, K. Moon, Y. Li, C.P. Wong, Chem. Mater. **18**, 2969 (2006)
20. M. Zulkarnain, M. Mariatti, I. Azid, J. Mater. Sci. Mater. Electron. **24**, 1523 (2012)
21. Y. Oh, K.Y. Chun, E. Lee, Y.J. Kim, S. Baik, J. Mater. Chem. **20**, 3579 (2010)
22. A. Mikrajuddin, F.G. Shi, S. Chungpaiboonpatana, K. Okuyama, C. Davidson, J.M. Adams, Mater. Sci. Semicond. Process. **2**, 309 (1999)
23. A.J. Lovinger, J. Adhes. **10**, 1 (1979)
24. H. Wu, X. Wu, M. Ge, G.Q. Zhang, Y.W. Wang, J.A. Jiang, Compos. Sci. Technol. **67**, 1116 (2007)
25. T. Yu, Z.G. Yang, X.L. Lu, G.L. Tao, Y.P. Xia, H.P. Wu, Sci. China Technol. Sci. **55**, 28 (2011)
26. J. Li, J.K. Lumpp, R. Andrews, D. Jacques, J. Adhes. Sci. Technol. **22**, 1659 (2008)
27. L. Li, J.E. Morris, IEEE Trans. Compon. Packag. Manuf. Technol. Part A **20**, 3 (1997)
28. C.A. Martin, J.K.W. Sandler, M.S.P. Shaffer, M.K. Schwarz, W. Bauhofer, K. Schulte, A.H. Windle, Compos. Sci. Technol. **64**, 2309 (2004)
29. J. Li, P.C. Ma, W.S. Chow, C.K. To, B.Z. Tang, J.K. Kim, Adv. Funct. Mater. **17**, 3207 (2007)
30. H. Jiang, K. Moon, J. Lu, J. Electron. Mater. **34**, 1432 (2005)
31. G.R. Ruschau, S. Yoshikawa, R.E. Newnham, J. Appl. Phys. **72**, 953 (1992)
32. M. Amjadi, A. Pichitpajongkit, S. Lee, S. Ryn, I. Park, ACS Nano **8**, 5154 (2014)
33. N. Hu, Y. Karube, C. Yan, Z. Masuda, H. Fukunaga, Acta Mater. **56**, 2929 (2008)
34. J.G. Simmons, J. Appl. Phys. **34**, 1793 (1963)
35. D. Lu, Q.K. Tong, C.P. Wong, Int. Symp. Adv. Packag. Mater. **22**, 365–371 (1999)
36. Y. Li, K. Moon, A. Whitman, C.P. Wong, IEEE Trans. Compon. Packag. Technol. **29**, 758 (2006)
37. C. Yang, Y.T. Xie, M.M.F. Yuen, B. Xu, B. Gao, X. Xiong, C.P. Wong, Adv. Funct. Mater. **20**, 2580 (2010)
38. C. Yang, W. Lin, Z. Li, R. Zhang, H. Wen, B. Gao, G. Chen, P. Gao, M.M.F. Yuen, C.P. Wong, Adv. Funct. Mater. **21**, 4582 (2011)
39. C. Gallagher, G. Matijasevic, J.F. Maguire, IEEE Electron. Compon. Technol. Conf. 554–560 (1997)
40. B.M. Amoli, S.A. Ramazani, H. Izadi, J. Appl. Polym. Sci. **125**, 453 (2012)
41. R. Zhang, K. Moon, W. Lin, C.P. Wong, J. Mater. Chem. **20**, 2018 (2010)
42. F. Marcq, P. Demont, P. Monfraix, A. Peigney, C. Laurent, T. Falat, F. Courtade, T. Jamin, Microelectron. Reliab. **51**, 1230 (2011)
43. H.L. Ma, H.B. Zhang, Q.H. Hu, W.J. Li, Z.G. Jiang, Z.Z. Yu, A.C.S. Appl, Mater. Interfaces **4**, 1948 (2012)
44. H.W. Cui, A. Kowalczyk, D.S. Li, Q. Fan, Int. J. Adhes. Adhes. **44**, 220 (2013)
45. Y. Long, J. Wu, H. Wang, X. Zhang, N. Zhao, J. Xu, J. Mater. Chem. **21**, 4875 (2011)
46. H.H. Lee, K.S. Chou, Z.W. Shih, Int. J. Adhes. Adhes. **25**, 437 (2005)
47. L. Fan, B. Su, J. Qu, C.P. Wong, Electron. Compon. Technol. Conf. 148–154 (2004)
48. P. Mach, R. Radev, A. Pietrikova, IEEE Electron. Syst. Technol. Conf. 1141–1146 (2008)
49. L. Ye, Z. Lai, J. Liu, IEEE Trans. Electron. Packag. Manuf. **22**, 299 (1999)
50. H. Gao, L. Liu, Y. Luo, D. Jia, Mater. Lett. **65**, 3529 (2011)
51. R. Zhang, W. Lin, K. Moon, C.P. Wong, ACS Appl. Mater. Interfaces **2**, 2637 (2010)
52. R. Zhang, K. Moon, W. Lin, J.C. Agar, C.P. Wong, Compos. Sci. Technol. **71**, 528 (2011)
53. A. Hu, J.Y. Guo, H. Alarifi, G. Patane, Y. Zhou, G. Compagnini, C.X. Xu, Appl. Phys. Lett. **97**, 153117 (2010)
54. D. Wakuda, K. Kim, K. Suganuma, Scr. Mater. **59**, 649 (2008)
55. S. Lai, J. Guo, V. Petrova, G. Ramanath, L.H. Allen, Phys. Rev. Lett. **77**, 99 (1996)
56. B.J. Perelaer, A.W.M. de Laat, C.E. Hendriks, U.S. Schubert, J. Mater. Chem. **18**, 3209 (2008)
57. Z.Z. Fang, H. Wang, Int. Mater. Rev. **53**, 326 (2008)
58. J.G. Bai, T.G. Lei, J.N. Calata, G.Q. Lu, J. Mater. Res. **22**, 3494 (2011)
59. P. Peng, A. Hu, H. Huang, A.P. Gerlich, B. Zhao, Y.N. Zhou, J. Mater. Chem. **22**, 12997 (2012)
60. S. Magdassi, M. Grouchko, O. Berezin, A. Kamyshny, ACS Nano **4**, 1943 (2010)
61. Y. Li, K. Moon, C.P. Wong, IEEE Electron. Compon. Technol. Conf. **29**, 173 (2006)
62. L. Polavarapu, K.K. Manga, H.D. Cao, K.P. Loh, Q.H. Xu, Chem. Mater. **23**, 3273 (2011)
63. T. Akter, W.S. Kim, ACS Appl. Mater. Interfaces **4**, 1855 (2012)
64. H.P. Wu, J.F. Liu, X.J. Wu, M.Y. Ge, Y.W. Wang, G.Q. Zhang, J.Z. Jiang, Int. J. Adhes. Adhes. **26**, 617 (2006)
65. Y.H. Yu, C.C.M. Ma, S.M. Yuen, C.C. Teng, Y.L. Huang, I. Wang, M.H. Wei, Macromol. Mater. Eng. **295**, 1017 (2010)
66. D. Chen, X. Qiao, X. Qiu, F. Tan, J. Chen, R. Jiang, J. Mater. Sci. Mater. Electron. **21**, 486 (2010)
67. Z. Zhang, X. Chen, H. Yang, H. Fu, F. Xiao, Int. Conf. Electron. Packag. Technol. High Density Packag. **107**, 6826–6829 (2009)
68. M. Moskovits, J.S. Suh, J. Am. Chem. Soc. **107**, 6826 (1985)
69. Z.X. Zhang, X.Y. Chen, F. Xiao, J. Adhes. Sci. Technol. **25**, 1465 (2011)
70. X. Yang, W. He, S. Wang, G. Zhou, Y. Tang, J. Mater. Sci. Mater. Electron. **23**, 108 (2011)
71. E. Marzbanrad, A. Hu, B. Zhao, Y. Zhou, J. Phys. Chem. C **117**, 16665 (2013)
72. B.M. Amoli, E. Marzbanrad, A. Hu, Y.N. Zhou, B. Zhao, Macromol. Mater. Eng. **299**, 739 (2014)
73. S. Iijima, Nature **354**, 56 (1991)
74. K.S. Novoselov, A.K. Geim, S.V. Morozov, D. Jiang, M.I. Katsnelson, I.V. Grigorieva, S.V. Dubonos, A.A. Firsov, Nature **438**, 197 (2005)
75. T.W. Odom, J. Huang, Nature **391**, 1997 (1998)
76. D.D. Lu, Y.G. Li, C.P. Wong, J. Adhes. Sci. Technol. **22**, 815 (2008)
77. E.E. Tkalya, M. Ghislandi, G. With, C.E. Koning, Curr. Opin. Colloid Interface Sci. **17**, 225 (2012)
78. A. O'Neill, U. Khan, P.N. Nirmalraj, J. Boland, J.N. Coleman, J. Phys. Chem. C **115**, 5422 (2011)
79. V.H. Pham, T.V. Cuong, S.H. Hur, E. Oh, E.J. Kim, E.W. Shin, J.S. Chung, J. Mater. Chem. **21**, 3371 (2011)

80. V.H. Luan, H.N. Tien, T.V. Cuong, B.S. Kong, J.S. Chung, E.J. Kim, S.H. Hur, J. Mater. Chem. **22**, 8649 (2012)
81. Y. Si, E.T. Samulski, Synthesis of water soluble graphene. Nano Lett. **8**, 1679 (2008)
82. A.S. Wajid, H.S.T. Ahmed, S. Das, F. Irin, A.F. Jankowski, M.J. Green, Macromol. Mater. Eng. **298**, 339 (2013)
83. L. Xuechun, L. Feng, in *Proceedings of the Sixth IEEE CPMT Conference in High Density Microsystem Des. Packag. Compon. Fail. Anal. (HDP '04)*. IEEE (2004), pp. 382–384
84. H. Wu, X. Wu, M. Ge, G.Q. Zhang, Y.W. Wang, J. Jiang, Compos. Sci. Technol. **67**, 1182 (2007)
85. Y. Oh, D. Suh, Y. Kim, E. Lee, J.S. Mok, J. Choi, S. Baik, Nanotechnology **19**, 495602 (2008)
86. N.W. Pu, Y.Y. Peng, P.C. Wang, Carbon **67**, 449 (2014)
87. X. Peng, F. Tan, W. Wang, X. Qiu, F. Sun, X. Qiao, J. Chen, J. Mater. Sci. Mater. Electron. **25**, 1149 (2014)
88. K. Liu, S. Chen, Y. Luo, D. Jia, H. Gao, G. Hu, L. Liu, Compos. Sci. Technol. **94**, 1 (2014)
89. K. Liu, L. Liu, Y. Luo, D. Jia, J. Mater. Chem. **22**, 20342 (2012)
90. K. Liu, S. Chen, Y. Luo, D. Jia, H. Gao, G. Ju, L. Liu, Compos. Sci. Technol. **88**, 84 (2013)
91. B.M. Amoli, J. Trinidad, A. Hu, Y.N. Zhou, B. Zhao, J. Mater. Sci. Mater. Electron. **26**, 590 (2014)